

Anomalous Shiba states in topological iron-based superconductors

Areg Ghazaryan,¹ Ammar Kirmani,² Rafael M. Fernandes,³ and Pouyan Ghaemi^{2,4}

¹*Institute of Science and Technology Austria, Am Campus 1, 3400 Klosterneuberg, Austria*

²*Physics Department, City College of the City University of New York, NY 10031, U.S.A.*

³*School of Physics and Astronomy, University of Minnesota, Minneapolis, Minnesota 55455, US*

⁴*Physics Program, Graduate Center of City University of New York, NY 10031, U.S.A.*

We demonstrate the formation of robust zero energy modes close to magnetic impurities in the iron-based superconductor $\text{FeSe}_{1-x}\text{Te}_x$. We find that the Zeeman field generated by the impurity favors a spin-triplet inter-orbital pairing as opposed to the spin-singlet intra-orbital pairing prevalent in the bulk. The preferred spin-triplet pairing preserves time-reversal symmetry and is topological, as robust, topologically-protected zero modes emerge at the boundary between regions with different pairing states. Moreover, the zero modes form Kramers doublets that are insensitive to the direction of the spin polarization or to the separation between impurities. We argue that our theoretical results are consistent with recent experimental measurements on $\text{FeSe}_{1-x}\text{Te}_x$.

Introduction: Topological superconductivity (TSc) is a quantum state that has been extensively explored [1–3], particularly due to its application for realizing Majorana zero modes (MZM) [4, 5]. In recent years, the iron-based superconductor $\text{FeSe}_{1-x}\text{Te}_x$ (FST) emerged as a promising candidate for TSc [6]. It was theoretically predicted that the band inversion in the electronic structure of FST can lead to localized MZM at the end of vortex lines in the superconducting phase [7]. One of the appeals of superconducting FST is the comparable energy scales between the superconducting gap and the Fermi energy, which leads to a wide spectral resolution of the vortex zero mode [8]. The experimental observation of such vortex zero modes has led to extensive studies of FST as a bulk TSc [9–13]. The interplay between topology, superconductivity and magnetism has also been investigated in relation to surface states and generating new superconducting order [14–19]. On the other hand, several of the properties of FST, such as the existence of vortices with and without zero modes in the same sample, have been puzzling [12, 20–23].

Another type of in-gap states in superconductors are the Shiba states, which form near magnetic impurities [24–26]. In certain regimes in-gap states can also be formed for non-magnetic impurity [27] even when the system respects time-reversal symmetry [28, 29]. In FST, in-gap states have been observed near interstitial Fe atoms [30], which behave as magnetic impurities [31]. Interestingly, several of the properties of these in-gap states are different from those of conventional Shiba states. First, Shiba states generally have a finite energy unless the microscopic properties of the superconductor and the coupling strength of the magnetic impurity with the itinerant electrons are fine tuned [32]. Yet in FST the in-gap states at many of the magnetic impurities are observed at zero energy [30, 33]. The other surprising property is the absence of a hybridization gap in the Shiba-state energies of two nearby magnetic impurities [30], which contrasts with the standard behavior seen in conventional systems [34]. STM measurements have further shown

that, while the energy of the in-gap state is zero when the impurity is at the center of the unit cell, it becomes finite when the impurity is pushed toward the edge of the unit cell [33]. Proposals such as anomalous quantum vortices forming at magnetic impurities [35] or effective π -phase shifts at the impurity sites [36, 37] have been put forward, but a comprehensive description of properties of these states is still lacking.

In this Letter we present an alternative mechanism for formation of zero energy states close to magnetic impurities in FST. The key property of FST leading to the type of in-gap states discussed in this Letter is the possible existence of multiple superconducting pairing instabilities energetically close to each other. Near an impurity, the Zeeman field generated by it strongly impacts this balance between different types of pairing. In particular, by solving the linearized gap equations, we find that the pairing state favored by the Zeeman field in this region is topologically distinct from the pairing state in regions farther than a multiple lattice spacing from the magnetic impurity. As a result, a pair of zero-energy states form in the boundary region between the two types of pairing. The resulting zero-energy states form bubbles surrounding the magnetic impurity, with a radius of the order of multiple lattice spacing. Since these states arise from the topological character of the superconducting state, their energy is generally pinned at zero.

When two impurities approach each other, the regions around them where the topological superconductivity is dominant merge. As a result, the zero modes surround a larger area and do not become gapped. Furthermore, the type of pairing that is preferred close to the impurity is determined by the symmetries of the system. Therefore, the position of the impurity in the unit cell can affect the type of pairing selected and, consequently, the development of zero modes. Interestingly, the triplet superconducting pairing that forms close to the magnetic impurity is time-reversal symmetric, and the boundary states are Kramers pairs that are insensitive to the direction of the spin-polarization of the magnetic impurity.

The later property is consistent with results from spin-polarized STM measurements [38]. Another feature of the magnetic-impurity induced in-gap state in FST is that it becomes gapped once the magnetic impurity approaches a magnetic vortex [33]. This is because the two zero modes enclosing the magnetic impurity hybridize in the presence of a Zeeman field. Therefore, due the vortex hosting a sizable magnetic field, it gaps out the zero modes.

Model Hamiltonian: FST is a member of the family of iron-based superconductors [39] with non-symmorphic $P4/nmm$ space group symmetry due to the buckling of the chalcogen atoms inside the 2-Fe unit cell [40–42]. At the Γ point, the $P4/nmm$ space group is isomorphic to the D_{4h} point group. The generators of the D_{4h} group can be taken to be π_x , π_z and π_X reflection planes. Here, x and y connect nearest-neighbor Fe atoms, whereas X and Y , rotated by 45° with respect to x and y , connect next-nearest-neighbor Fe atoms. The FeSe layers are stacked along z . The band structure close to Γ point mainly contains p_z , d_{xz} and d_{yz} orbitals and the most general effective Hamiltonian including spin-orbit coupling (SOC) can be constructed using the method of invariants [43, 44]. The inversion-odd p_z orbital is essential for realizing band inversion along the $\Gamma - Z$ direction and thus the nontrivial topology of the band structure [7, 42]. In the basis $\psi_{\mathbf{k}} = (|d_+ \uparrow\rangle, |d_- \uparrow\rangle, |p_z \uparrow\rangle, |d_+ \downarrow\rangle, |d_- \downarrow\rangle, |p_z \downarrow\rangle)$, where $d_{\pm} = (d_{yz} \pm id_{xz})^T$, the Hamiltonian is given by [42]

$$H(\mathbf{k}) = \sigma_0 \otimes H_0(\mathbf{k}) + H_{\text{SOC}}(\mathbf{k}), \quad (1)$$

where for small in-plane momentum:

$$H_0(\mathbf{k}) = \begin{pmatrix} M_1(\mathbf{k}) & \beta k_+^2 & \delta k_- \\ \beta k_-^2 & M_1(\mathbf{k}) & -\delta k_+ \\ \delta k_+ & -\delta k_- & M_2(\mathbf{k}) \end{pmatrix}, \quad (2)$$

with $k_{\pm} = k_x \pm ik_y$ and $M_n(\mathbf{k}) = E_n + (k_x^2 + k_y^2)/2m_{n_x} + t_{n_z}(1 - \cos(k_z))$.

The non-zero elements of the SOC Hamiltonian $H_{\text{SOC}}(\mathbf{k})$ are $H_{\text{SOC}}^{22}(\mathbf{k}) = H_{\text{SOC}}^{44}(\mathbf{k}) = -H_{\text{SOC}}^{11}(\mathbf{k}) = -H_{\text{SOC}}^{55}(\mathbf{k}) = \lambda_1$, and $H_{\text{SOC}}^{16}(\mathbf{k}) = H_{\text{SOC}}^{35}(\mathbf{k}) = \sqrt{2}\lambda_3 \sin(k_z)$, as well as the matrix elements related by hermiticity. The parameters β , δ , E_1 , E_2 , m_1 , m_2 , t_1 , t_2 , λ_1 and λ_3 were previously determined using density functional theory [7]. *Symmetries and pairing states:* The types of pairing states in FST can be classified according to irreducible representations of the D_{4h} symmetry group of the underlying lattice [45]. D_{4h} has five odd-parity and five even-parity irreducible representations. We only consider pairing with zero center-of-mass momentum. In the even sector, the standard pairing is intra-orbital spin-singlet that transforms as the A_{1g} representation and has the form $\Delta_1 : \sigma_0 \otimes \mathbf{1}_3$. We use the standard BdG basis where the wave function has the form $\Psi_{\mathbf{k}} = (\psi_{\mathbf{k}}, i\sigma_y K \psi_{\mathbf{k}})^T$. Due to the presence of SOC,

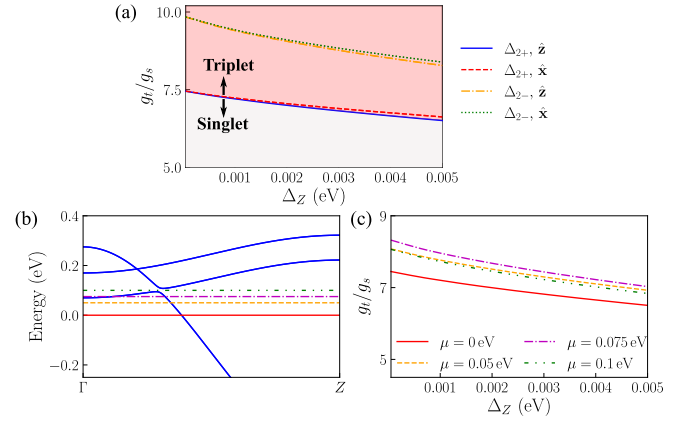


FIG. 1. (a) Phase boundary between different inter-orbital triplet ($\Delta_{2\pm}$) and intra-orbital spin-singlet (Δ_1) pairing states for $\mu = 0$ eV when the Zeeman field is along the \hat{z} or \hat{x} direction. Singlet (triplet) pairing emerges in the light gray (light red) region, following the phase boundary for the Zeeman field along the \hat{z} direction. (b) Band structure in the $\Gamma - Z$ direction. The selected chemical potentials are those for which the phase boundaries between Δ_{2+} and Δ_1 are shown in (c). The Zeeman field is in the \hat{z} direction for (c).

there is a spin-triplet inter-orbital pairing involving the d_{xz} and d_{yz} orbitals that also transforms as A_{1g} , of the form $\sigma_z d_{xz} d_{yz}$. This pairing state, favored by the Hund's coupling [46], does not pair the p_z orbitals. Therefore, when the chemical potential is close to the p - d band inversion point, $\sigma_z d_{xz} d_{yz}$ pairing state is not energetically favorable.

On the other hand, there are four types of odd-parity pairing states that are inter-orbital triplet and involve the p_z orbital. They are $\Delta_{2\pm} : \sigma_x p_z d_{xz} \pm \sigma_y p_z d_{yz}$, which transforms as the A_{1u} (+) or B_{1u} (-) irreducible representation; and $\Delta_{3\pm} : \sigma_y p_z d_{xz} \mp \sigma_x p_z d_{yz}$, which transforms as A_{2u} (+) or B_{3u} (-). In the d_{\pm} basis, these gap functions generate the Bogoliubov-de Gennes mean-field pairing terms:

$$H_{\Delta_{\{2,3\},+}} = \Delta_{\{2,3\},+} i^{\{0,1\}} \tau_x \begin{pmatrix} 0 & 0 & 0 & 0 & 0 & 1 \\ 0 & 0 & 0 & 0 & 0 & 0 \\ 0 & 0 & 0 & 0 & -1 & 0 \\ 0 & 0 & 0 & 0 & 0 & 0 \\ 0 & 0 & \mp 1 & 0 & 0 & 0 \\ \pm 1 & 0 & 0 & 0 & 0 & 0 \end{pmatrix}, \quad (3)$$

$$H_{\Delta_{\{2,3\},-}} = \Delta_{\{2,3\},-} i^{\{0,1\}} \tau_x \begin{pmatrix} 0 & 0 & 0 & 0 & 0 & 0 \\ 0 & 0 & 0 & 0 & 0 & 1 \\ 0 & 0 & 0 & -1 & 0 & 0 \\ 0 & 0 & \mp 1 & 0 & 0 & 0 \\ 0 & 0 & 0 & 0 & 0 & 0 \\ 0 & \pm 1 & 0 & 0 & 0 & 0 \end{pmatrix}, \quad (4)$$

where the upper (lower) signs refer to Δ_2 (Δ_3) and the Pauli matrix τ_j acts in Nambu particle-hole space. The

overall phase was chosen such that both $\Delta_{2,\pm}$ and $\Delta_{3,\pm}$ respect time-reversal symmetry.

From numerical analysis, we identify that all these pairing states, except Δ_{2+} , are nodal. The novel structure of the pairing gaps has important implications for the topological character of the superconducting state. Indeed, a time-reversal and odd-parity pairing is topological if it is gapped and encloses an odd number of time-reversal invariant momenta [47]. The space group $P4/nmm$ has the non-symmorphic symmetry operation inversion followed by half translation, which at the Γ point corresponds to the inversion symmetry operation of D_{4h} [41]. As a result, the triplet pairings of FST identified above, $\Delta_{2\pm}$ and $\Delta_{3\pm}$, have odd parity. Since only Δ_{2+} has a full gap, it is the only one among those four that can be in a topological superconducting state, as long as it encloses an odd number of time-reversal invariant momenta.

Effect of the Zeeman field: To determine the dominant pairing instability as a function of the Zeeman field we utilize the linearized gap equation [48]. We start by defining the finite temperature superconducting susceptibilities:

$$\chi_{lm} = -\frac{T}{N} \sum_{\omega_n, \mathbf{p}} \text{Tr} \left[\frac{H_{\Delta_l}^\dagger}{\Delta_l} G_0(i\omega_n, \mathbf{p}, \Delta_Z) \times \frac{H_{\Delta_m}}{\Delta_m} G_0(-i\omega_n, \mathbf{p}, -\Delta_Z) \right], \quad (5)$$

where H_{Δ_l} is the pairing Hamiltonian, N is the number of momentum points, and $G_0(i\omega_n, \mathbf{p}, \Delta_Z) = \sum_j \mathcal{P}_{j\mathbf{p}\Delta_Z} / (i\omega_n - \epsilon_{j\mathbf{p}\Delta_Z})$ is the normal state Green's function. j runs through the bands, ω_n is the Matsubara frequencies and $\mathcal{P}_{j\mathbf{p}\Delta_Z}$ is the projection operator onto band j at momentum \mathbf{p} . The Zeeman-field energy splitting is Δ_Z . Finally, the subscripts l and m label the five pairing states discussed above: the singlet Δ_1 and the triplets $\Delta_{2\pm}$, $\Delta_{3\pm}$. The linearized gap equations, which determine the critical temperature T_c for each pairing instability, take the form

$$-\frac{1}{g_s} - \chi_{11} = 0, \quad (6)$$

$$-\frac{2}{3g_t} - \chi_{tt} = 0, \quad (7)$$

where g_l are the superconducting coupling constants arising from the microscopic interactions, with $s = 1$ and $t = \pm 2, \pm 3$. In deriving these expressions, we ignored mixing between different pairing channels, e.g. Δ_{2+} and Δ_{2-} , that is allowed by the Zeeman field. We will justify this later.

To proceed, we need to discuss the coupling constants g_l . We assume, without specifying a mechanism, that there is attractive interaction in the singlet channel, since this is the state realized in the bulk. As for the triplet

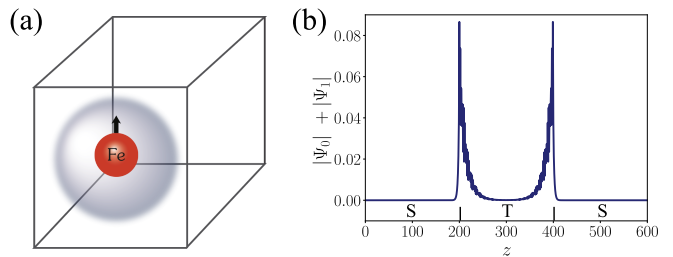


FIG. 2. (a) Schematic representation of the interstitial Fe atom and its surrounding triplet pairing state, separated from the spin-singlet pairing realized away from the atom. (b) Corresponding total probability distribution, along the \hat{z} direction, for the zero-energy mode Kramers pair. The system size is 600 lattice sites, divided into three regions of singlet/triplet (topological)/singlet pairings with 200 sites each. The chemical potential is $\mu = 0$ meV, and $k_x = k_y = 0$.

states, according to what we discussed above, only Δ_{2+} can correspond to a topological pairing state, which can display zero-energy modes. It is therefore crucial to identify the microscopic interactions that favors $g_{2\pm}$ over $g_{3\pm}$. We start from a generalized Hubbard-Kanamori interacting Hamiltonian [49–51] for the p_z , d_{xz} , and d_{yz} orbitals, which includes anisotropic Hund's terms J_1 , J_2 and J_3 . We find a simple condition under which there is an effective attractive interaction only for the $\Delta_{2\pm}$ states (see Supplementary Information): $J_1 > J_2$ and $J_3 + J_1 - J_2 < V < J_3 + J_2 - J_1$, where V is the inter-orbital Hubbard repulsion. We assume this condition is satisfied, set $g_{2\pm} = g_t$, and focus hereafter on the $\Delta_{2\pm}$ and Δ_1 states only.

Fig. 1 (a) shows the phase boundaries for the different pairing states in the parameter space of Zeeman splitting and the coupling constants ratio g_t/g_s . The Zeeman field is taken in the \hat{z} or \hat{x} (in-plane) direction. The phase boundaries between Δ_{2+} and Δ_{2-} are quite separated, such that Δ_{2+} dominates for small values of the coupling constant ratio, regardless of the field direction. This not only shows that Δ_{2+} is the favored pairing state for larger Zeeman coupling, but also that the Zeeman-induced mixing with Δ_{2-} should be small, which justifies dropping this term in the gap equations. Fig. 1 (a) shows that phase boundary is almost insensitive to the direction of the Zeeman field.

To show that Δ_{2+} pairing is robust with respect to changes in the chemical potential, Fig. 1 (b,c) shows the small changes experienced by the Δ_{2+} - Δ_1 phase boundary for four different values of μ . Therefore, upon increasing the Zeeman coupling, the pairing state will transition from intra-orbital singlet Δ_1 to inter-orbital triplet Δ_{2+} .

While the preferred pairing is robust with respect to the chemical potential modification, its topological nature depends on the chemical potential. The relevant time-reversal invariant momenta are at the Γ and Z points. For $\mu > -0.577$ eV, the Fermi surface at the

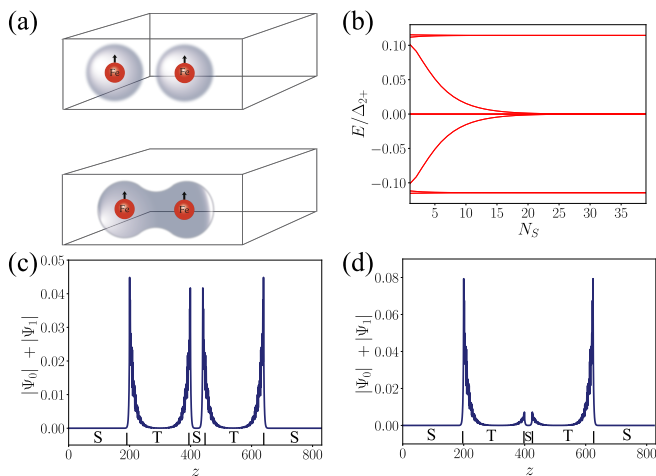


FIG. 3. (a) Schematic representation of bringing two interstitial Fe atoms closer. (b) Dependence of the in-gap energy states on the effective two impurity separation in the \hat{z} direction. The two impurity state is simulated by a five region sandwich with superconducting pairings singlet/triplet/singlet/triplet/singlet; the distance between the boundaries of the two triplet regions is N_S sites. (c,d) Corresponding total probability when two Fe atoms are farther apart and closer to each other, respectively. For (c,d) the system is the same as in (b) with $N_S = 25$ for (c) and $N_S = 40$ for (d). Chemical potential is $\mu = 0$ meV and $k_x = k_y = 0$.

Z point is filled whereas for $\mu < 0.07$ eV, all three bands at Γ are empty. Therefore, in this range of μ , the Δ_{2+} pairing state is topological. Consequently, in Fig. 1 (c,d), only two chemical potential values $\mu = 0$ eV and $\mu = 0.05$ eV correspond to a topological superconductor. The cases $\mu = 0.075$ eV and $\mu = 0.1$ eV are generally non-topological. For $\mu = 0.075$ eV, the lowest band at the Γ point is quite close to the Fermi energy. As a result, a topological phase transition can be induced by increasing the pairing amplitude or further tuning the chemical potential. Since this requires considerable tuning, difficult to achieve experimentally, we focus on values of the chemical potential where Δ_{2+} is strictly topological.

When the chemical potential is in the band-inversion gap, the normal-state itself is topological [7] (see Fig. 1 (c)). This is manifested by Majorana bound states at the end of the vortex cores where they cross the sample boundary [10, 52]. In this case, the bulk pairing state is intra-orbital spin-singlet Δ_1 which is not topological in the bulk, but it also induces topological superconductivity on the surface [52]. Since our interest is in the vicinity of bulk impurities, we will not discuss surface effects.

Majorana modes: Having identified the dominant pairing state in the presence of Zeeman coupling, we now examine the possible boundary mode localized between regions with Δ_{2+} and spin-singlet Δ_1 pairings. Since for a considerable range of chemical potential values the Δ_{2+} pairing is topological, the presence of zero-energy edge modes is expected. The Δ_{2+} pairing respects time-

reversal symmetry, therefore the zero modes are Kramers pairs with opposite spin.

Figs. 2 and 3 depict the structure of zero modes for single and double magnetic impurities. Figs. 2 (a) and (b) show the case of a single Fe impurity. The effective magnetic field generated by the magnetic impurity modifies the superconducting order parameter in its surroundings, such that Δ_{2+} pairing is realized. The boundary with the bulk singlet pairing features zero energy modes. Therefore, scanning tunneling spectroscopy close to the interstitial iron atom should detect a robust zero bias peak [30, 33, 38]. The observed zero mode is different from usual Shiba state observed next to a magnetic impurity [53], whose energy depends on the amplitude of the exchange interaction and requires special tuning to be fixed at zero energy. In contrast, in our case, as long as the magnetic field is sufficiently large to favor topological Δ_{2+} pairing, the zero-energy mode is robust.

Fig. 3 shows the evolution of the zero modes when the two impurities are brought close to each other. As shown in Fig. 3 (b), while two of the zero modes are gapped out, the ones located on the outer edge of the two-impurity region remain robust. This is consistent with the experimental observation in Ref. [30] and is different from the expected hybridization between Shiba states when the two impurities are brought close to each other. This shows that the corresponding zero modes form bubbles around the magnetic impurities, which combine into a single bubble enclosing both atoms when the impurities are close to each other.

Finally, we comment on the size of the bubble formed around the interstitial magnetic impurity. Analyzing the Friedel oscillations from neutron scattering data, Ref. [31] used a five-orbital Hubbard model to estimate that the nearest-neighbor spin exchange between the interstitial and the surrounding Fe atoms is about 70 meV. This is an order of magnitude larger than the Zeeman field required to observe the triplet pairing state and the topological superconducting region around the magnetic impurity (see Fig. 1). Therefore, despite the exchange interaction being short-ranged, we expect the radius of the bubble to be in the range of a multiple lattice spacing, consistent with experimental observations [30].

conclusions: We have shown that the peculiar features of the zero bias peak experimentally observed at interstitial iron atoms in FST can be reconciled if we consider the modification of the superconducting order parameter close to the impurity. We have shown that the Zeeman field prefers inter-orbital triplet pairing which, for a certain range of chemical potential values, is topological. As a result, zero-energy modes naturally occur at the boundary between inter-orbital triplet and intra-orbital singlet pairings. These modes are robust and do not get modified by changes in the exchange interaction, contrary to the conventional Shiba states. It has been experimentally observed that the zero modes are not spin-polarized [38], a

feature that is also consistent with our theoretical model. The obtained triplet pairing state near the impurity respects time-reversal symmetry, such that the zero modes are always doubly-degenerate and have opposite spin due to the Kramers theorem. This mechanism is also capable of explaining the robustness of the zero modes when two impurities are brought close to each other, since in this case only two out of four modes get hybridized.

We thank Armin Rahmani, Andrey V. Chubukov, Jay D. Sau and Ruixing Zhang for fruitful discussions. AK and PG are supported by NSF-DMR2037996. PG also acknowledges support from NSF-DMR1824265. RMF was supported by the U. S. Department of Energy, Office of Science, Basic Energy Sciences, Materials Sciences and Engineering Division, under Award No. DE-SC0020045. Part of this work was performed at the Aspen Center for Physics, which is supported by National Science Foundation grant PHY-1607611.

-
- [1] M Zahid Hasan and Charles L Kane, “Colloquium: topological insulators,” *Rev. Mod. Phys.* **82**, 3045 (2010).
- [2] Xiao-Liang Qi and Shou-Cheng Zhang, “Topological insulators and superconductors,” *Rev. Mod. Phys.* **83**, 1057 (2011).
- [3] Masatoshi Sato and Yoichi Ando, “Topological superconductors: a review,” *Rep. Prog. Phys.* **80**, 076501 (2017).
- [4] Jason Alicea, “New directions in the pursuit of majorana fermions in solid state systems,” *Reports on Progress in Physics* **75**, 076501 (2012).
- [5] Karsten Flensberg, Felix von Oppen, and Ady Stern, “Engineered platforms for topological superconductivity and majorana zero modes,” *Nature Reviews Materials* **6**, 944–958 (2021).
- [6] Zhijun Wang, Peng Zhang, Gang Xu, LK Zeng, Hu Miao, Xiaoyan Xu, Tian Qian, Hongming Weng, P Richard, Alexei V Fedorov, H. Ding, Xi Dai, and Zhong Fang, “Topological nature of the $\text{fese}_{0.5}\text{te}_{0.5}$ superconductor,” *Phys. Rev. B* **92**, 115119 (2015).
- [7] Gang Xu, Biao Lian, Peizhe Tang, Xiao-Liang Qi, and Shou-Cheng Zhang, “Topological superconductivity on the surface of fe-based superconductors,” *Physical review letters* **117**, 047001 (2016).
- [8] Andreas Kreisel, Peter J Hirschfeld, and Brian M Andersen, “On the remarkable superconductivity of fese and its close cousins,” *Symmetry* **12**, 1402 (2020).
- [9] Peng Zhang, Koichiro Yaji, Takahiro Hashimoto, Yuichi Ota, Takeshi Kondo, Kozo Okazaki, Zhijun Wang, Jinsheng Wen, GD Gu, Hong Ding, and Shik Shin, “Observation of topological superconductivity on the surface of an iron-based superconductor,” *Science* **360**, 182–186 (2018).
- [10] Dongfei Wang, Lingyuan Kong, Peng Fan, Hui Chen, Shiyu Zhu, Wenyao Liu, Lu Cao, Yujie Sun, Shixuan Du, John Schneeloch, Ruidan Zhong, Genda Gu, Liang Fu, Hong Ding, and Hong-Jun Gao, “Evidence for majorana bound states in an iron-based superconductor,” *Science* **362**, 333–335 (2018).
- [11] Shiyu Zhu, Lingyuan Kong, Lu Cao, Hui Chen, Michał Papaj, Shixuan Du, Yuqing Xing, Wenyao Liu, Dongfei Wang, Chengmin Shen, Fazhi Yang, John Schneeloch, Ruidan Zhong, Genda Gu, Liang Fu, Yu-Yang Zhang, Hong Ding, and Hong-Jun Gao, “Nearly quantized conductance plateau of vortex zero mode in an iron-based superconductor,” *Science* **367**, 189–192 (2020).
- [12] T Machida, Y Sun, S Pyon, S Takeda, Y Kohsaka, T Hanaguri, T Sasagawa, and T Tamegai, “Zero-energy vortex bound state in the superconducting topological surface state of fe (se, te),” *Nat. Mat.* **18**, 811–815 (2019).
- [13] Hu Miao, WH Brito, ZP Yin, RD Zhong, GD Gu, PD Johnson, MPM Dean, S Choi, G Kotliar, W Ku, X. C. Wang, C. Q. Jin, S.-F. Wu, T. Qian, and H. Ding, “Universal 2δ max/k b t c scaling decoupled from the electronic coherence in iron-based superconductors,” *Physical Review B* **98**, 020502 (2018).
- [14] Yangmu Li, Nader Zaki, Vasile O Garlea, Andrei T Savici, David Fobes, Zhijun Xu, Fernando Camino, Cedomir Petrovic, Genda Gu, Peter D Johnson, John M. Tranquada, and Igor A. Zaliznyak, “Electronic properties of the bulk and surface states of fe1+ yte1- xsex ,” *Nature Materials* **20**, 1221–1227 (2021).
- [15] Lun-Hui Hu, PD Johnson, and Congjun Wu, “Pairing symmetry and topological surface state in iron-chalcogenide superconductors,” *Physical Review Research* **2**, 022021 (2020).
- [16] Nader Zaki, Genda Gu, Alexei Tsvetlik, Congjun Wu, and Peter D Johnson, “Time-reversal symmetry breaking in the fe-chalcogenide superconductors,” *Proceedings of the National Academy of Sciences* **118**, e2007241118 (2021).
- [17] Cody Youmans, Areg Ghazaryan, Mehdi Kargarian, and Pouyan Ghaemi, “Odd-frequency pairing in the edge states of superconducting pnictides in the coexistence phase with antiferromagnetism,” *Physical Review B* **98**, 144517 (2018).
- [18] Maxim Dzero and Alex Levchenko, “Impurity bands in magnetic superconductors with spin density wave,” *Annals of Physics* , 168945 (2022).
- [19] Shaozi Li, Lun-Hui Hu, Rui-Xing Zhang, and Satoshi Okamoto, “Topological superconductivity from forward phonon scatterings,” *arXiv* : , 2207.09443 (2022).
- [20] Zhenyu Wang, Jorge Olivares Rodriguez, Lin Jiao, Sean Howard, Martin Graham, G. D. Gu, Taylor L. Hughes, Dirk K. Morr, and Vidya Madhavan, “Evidence for dispersing 1d majorana channels in an iron-based superconductor,” *Science* **367**, 104 (2020).
- [21] Ching-Kai Chiu, T Machida, Yingyi Huang, T Hanaguri, and Fu-Chun Zhang, “Scalable majorana vortex modes in iron-based superconductors,” *Sci. Adv.* **6**, eaay0443 (2020).
- [22] Areg Ghazaryan, Pedro LS Lopes, Pavan Hosur, Matthew J Gilbert, and Pouyan Ghaemi, “Effect of zeeman coupling on the majorana vortex modes in iron-based topological superconductors,” *Phys. Rev. B* **101**, 020504 (2020).
- [23] Lun-Hui Hu and Rui-Xing Zhang, “Topological superconducting vortex from trivial electronic bands,” (2022), arXiv:2204.03175.
- [24] Luh Yu, “Bound state in superconductors with paramagnetic impurities,” *Acta Phys. Sin.* **21**, 75 (1965).
- [25] H. Shiba, “Classical spins in superconductors,” *Classical Spins in Superconductors* **40**, 435 (1968).
- [26] A. I. Rusinov, “Superconductivity near paramagnetic im-

- purity,” JETP Lett. **9**, 85 (1969).
- [27] Jay D Sau and Eugene Demler, “Bound states at impurities as a probe of topological superconductivity in nanowires,” *Physical Review B* **88**, 205402 (2013).
- [28] Masashige Matsumoto, Mikito Koga, and Hiroaki Kusunose, “Single impurity effects in multiband superconductors with different sign order parameters,” *Journal of the Physical Society of Japan* **78**, 084718 (2009).
- [29] Mahdi Mashkooi, AG Moghaddam, MH Hajibabae, Annica M Black-Schaffer, and Fariborz Parhizgar, “Impact of topology on the impurity effects in extended s-wave superconductors with spin-orbit coupling,” *Physical Review B* **99**, 014508 (2019).
- [30] Jia-Xin Yin, Zheng Wu, J.H. Wang, Z.Y. Ye, Jing Gong, X.Y. Hou, Lei Shan, Ang Li, X.J. Liang, X.X. Wu, Jian Li, C.S. Ting, Z.Q. Wang, J.P. Hu, P.H. Hor, H. Ding, and S.H. Pan, “Observation of a robust zero-energy bound state in iron-based superconductor $\text{Fe}(\text{Te}, \text{Se})$,” *Nature Phys.* **11**, 543–546 (2015).
- [31] V. Thampy, J. Kang, J. A. Rodriguez-Rivera, W. Bao, A. T. Savici, J. Hu, T. J. Liu, B. Qian, D. Fobes, Z. Q. Mao, C. B. Fu, W. C. Chen, Q. Ye, R. W. Erwin, T. R. Gentile, Z. Tesanovic, and C. Broholm, “Friedel-like oscillations from interstitial iron in superconducting $\text{Fe}_{1+y}\text{Te}_{0.62}\text{Se}_{0.38}$,” *Phys. Rev. Lett.* **108**, 107002 (2012).
- [32] A. V. Balatsky, I. Vekhter, and Jian-Xin Zhu, “Impurity-induced states in conventional and unconventional superconductors,” *Rev. Mod. Phys.* **78**, 373–433 (2006).
- [33] Peng Fan, Fazhi Yang, Guojian Qian, Hui Chen, Yu-Yang Zhang, Geng Li, Zihao Huang, Yuqing Xing, Lingyuan Kong, Wenyao Liu, Kun Jiang, Chengmin Shen, Shixuan Du, John Schneeloch, Ruidan Zhong, Genda Gu, Ziqiang Wang, Hong Ding, and Hong-Jun Gao, “Observation of magnetic adatom-induced majorana vortex and its hybridization with field-induced majorana vortex in an iron-based superconductor,” *Nature comm.* **12**, 1–7 (2021).
- [34] Michael Ruby, Benjamin W. Heinrich, Yang Peng, Felix von Oppen, and Katharina J. Franke, “Wave-function hybridization in yu-shiba-rusinov dimers,” *Phys. Rev. Lett.* **120**, 156803 (2018).
- [35] Kun Jiang, Xi Dai, and Ziqiang Wang, “Quantum anomalous vortex and majorana zero mode in iron-based superconductor $\text{Fe}(\text{Te}, \text{Se})$,” *Phys. Rev. X* **9**, 011033 (2019).
- [36] Rui Song, Ping Zhang, Xian-Tu He, and Ning Hao, “Ferromagnetic impurity induced majorana zero mode in iron-based superconductor,” (2022), arXiv:2203.14017.
- [37] Kristofer Björnson, Alexander V Balatsky, and Annica M Black-Schaffer, “Superconducting order parameter π -phase shift in magnetic impurity wires,” *Physical Review B* **95**, 104521 (2017).
- [38] Dongfei Wang, Jens Wiebe, Ruidan Zhong, Genda Gu, and Roland Wiesendanger, “Spin-polarized yu-shiba-rusinov states in an iron-based superconductor,” *Phys. Rev. Lett.* **126**, 076802 (2021).
- [39] Rafael M Fernandes, Amalia I Coldea, Hong Ding, Ian R Fisher, PJ Hirschfeld, and Gabriel Kotliar, “Iron pnictides and chalcogenides: a new paradigm for superconductivity,” *Nature* **601**, 35–44 (2022).
- [40] Rafael M Fernandes and Andrey V Chubukov, “Low-energy microscopic models for iron-based superconductors: a review,” *Rep. Prog. Phys.* **80**, 014503 (2016).
- [41] Vladimir Cvetkovic and Oskar Vafek, “Space group symmetry, spin-orbit coupling, and the low-energy effective hamiltonian for iron-based superconductors,” *Phys. Rev. B* **88**, 134510 (2013).
- [42] Himanshu Lohani, Tamaghna Hazra, Amit Ribak, Yuval Nitzav, Huixia Fu, Binghai Yan, Mohit Randeria, and Amit Kanigel, “Band inversion and topology of the bulk electronic structure in $\text{FeSe}_{0.45}\text{Te}_{0.55}$,” *Phys. Rev. B* **101**, 245146 (2020).
- [43] Teturo Inui, Yukito Tanabe, and Yositaka Onodera, *Group theory and its applications in physics*, Vol. 78 (Springer-Verlag, Berlin, Heidelberg, 1990).
- [44] G. L. Bir, G. E. Pikus, *et al.*, *Symmetry and strain-induced effects in semiconductors*, Vol. 484 (John Wiley & Sons, New York, 1974).
- [45] Manfred Sigrist and Kazuo Ueda, “Phenomenological theory of unconventional superconductivity,” *Rev. Mod. Phys.* **63**, 239–311 (1991).
- [46] Oskar Vafek and Andrey V Chubukov, “Hund interaction, spin-orbit coupling, and the mechanism of superconductivity in strongly hole-doped iron pnictides,” *Phys. Rev. Lett.* **118**, 087003 (2017).
- [47] Liang Fu and Erez Berg, “Odd-parity topological superconductors: theory and application to $\text{Cu}_x\text{Bi}_2\text{Se}_3$,” *Physical review letters* **105**, 097001 (2010).
- [48] Mark H Fischer, “Gap symmetry and stability analysis in the multi-orbital Fe-based superconductors,” *New Journal of Physics* **15**, 073006 (2013).
- [49] Junjiro Kanamori, “Electron Correlation and Ferromagnetism of Transition Metals,” *Progress of Theoretical Physics* **30**, 275–289 (1963), <https://academic.oup.com/ptp/article-pdf/30/3/275/5278869/30-3-275.pdf>.
- [50] Antoine Georges, Luca de’ Medici, and Jernej Mravlje, “Strong correlations from Hund’s coupling,” *Annual Review of Condensed Matter Physics* **4**, 137–178 (2013).
- [51] Siegfried Graser, TA Maier, PJ Hirschfeld, and DJ Scalapino, “Near-degeneracy of several pairing channels in multiorbital models for the Fe pnictides,” *New J. Phys.* **11**, 025016 (2009).
- [52] Liang Fu and C. L. Kane, “Superconducting proximity effect and majorana fermions at the surface of a topological insulator,” *Phys. Rev. Lett.* **100**, 096407 (2008).
- [53] Alexander V Balatsky, Ilya Vekhter, and Jian-Xin Zhu, “Impurity-induced states in conventional and unconventional superconductors,” *Reviews of Modern Physics* **78**, 373 (2006).

**Supplementary material for:
“Anomalous Shiba states in topological iron-based superconductors”**

Areg Ghazaryan,¹ Ammar Kirmani,² Rafael M. Fernandes,³ and Pouyan Ghaemi^{2,4}

¹*Institute of Science and Technology Austria, Am Campus 1, 3400 Klosterneuburg, Austria*

²*Physics Department, City College of the City University of New York, NY 10031, U.S.A.*

³*School of Physics and Astronomy, University of Minnesota, Minneapolis, Minnesota 55455, US*

⁴*Physics Program, Graduate Center of City University of New York, NY 10031, U.S.A.*

PAIRING FROM INTERACTING HAMILTONIAN

Here we establish the relationship between the superconducting coupling constants $g_{2\pm}$ and $g_{3\pm}$ of the odd-parity pairing states discussed in the main text and the onsite interaction terms of a generalized Hubbard-Kanamori Hamiltonian [1–3] for the three orbitals d_{xz} , d_{yz} and p_z :

$$\begin{aligned}
 H_{int} = & U \sum_{i\mu} n_{i\mu\uparrow} n_{i\mu\downarrow} + \frac{V}{2} \sum_{i\mu\mu' \neq \mu} n_{i\mu} n_{i\mu'} - \frac{J_1}{2} \left(\sum_{i,\mu \neq \mu' = d_{xz}, p_z} S_{x,i\mu} S_{x,i\mu'} + \sum_{i,\mu \neq \mu' = d_{yz}, p_z} S_{y,i\mu} S_{y,i\mu'} \right) - \\
 & \frac{J_2}{2} \left(\sum_{i,\mu \neq \mu' = d_{xz}, p_z} S_{y,i\mu} S_{y,i\mu'} + \sum_{i,\mu \neq \mu' = d_{yz}, p_z} S_{x,i\mu} S_{x,i\mu'} \right) - \frac{J_3}{2} \left(\sum_{i,\mu \neq \mu' = d_{xz}, p_z} S_{z,i\mu} S_{z,i\mu'} + \sum_{i,\mu \neq \mu' = d_{yz}, p_z} S_{z,i\mu} S_{z,i\mu'} \right) - \\
 & \frac{J_d}{2} \left(\sum_{i,\mu \neq \mu' = d_{xz}, d_{yz}} S_{x,i\mu} S_{x,i\mu'} + \sum_{i,\mu \neq \mu' = d_{xz}, d_{yz}} S_{y,i\mu} S_{y,i\mu'} \right) - \frac{J_{dz}}{2} \sum_{i,\mu \neq \mu' = d_{xz}, d_{yz}} S_{z,i\mu} S_{z,i\mu'} + \frac{J'}{2} \sum_{i\mu \neq \mu' s} \mu_{is}^\dagger \mu_{i\bar{s}}^\dagger \mu_{i\bar{s}}' \mu_{is}',
 \end{aligned} \tag{S1}$$

where U and V describe the intra- and inter-orbital Hubbard interactions; J_1 , J_2 , J_3 describe the Hund's interactions between d_{xz} and p_z or d_{yz} and p_z orbitals; J_d and J_{dz} denote the Hund's interactions between the d_{xz} and d_{yz} orbitals; and J' describes the pair-hopping interaction. Here $n_{i\mu} = n_{i\mu\uparrow} + n_{i\mu\downarrow}$, \bar{s} denotes the opposite spin to s , and the density and spin operators are defined as usual

$$n_{i\mu s} = \mu_{is}^\dagger \mu_{is}, \tag{S2}$$

$$\mathbf{S}_{i\mu} = \frac{1}{2} \sum_{s,s'} \mu_{i,s}^\dagger \boldsymbol{\sigma}_{ss'} \mu_{i,s'}. \tag{S3}$$

Note that, in Eq. (S1), we consider the most general Hund's interactions allowed by C_4 symmetry and spin-orbit coupling. As a result, there are different Hund's couplings depending on the spin polarization and on the orbitals involved. This is necessary to distinguish between the four odd-parity superconducting states. Their gap functions can be written explicitly as

$$A_{1u} : \Delta_{2+} = g_{2+} \sum_{s,s'} \langle p_{zs} (i\sigma_x \sigma_y)_{ss'} d_{xz,s'} + p_{z,s} (i\sigma_y \sigma_y)_{ss'} d_{yz,s'} \rangle = g_{2+} \sum_{s,s'} \langle -p_{zs} \sigma_{z,ss'} d_{xz,s'} + ip_{z,s} \sigma_{0,ss'} d_{yz,s'} \rangle, \tag{S4}$$

$$B_{1u} : \Delta_{2-} = g_{2-} \sum_{s,s'} \langle p_{zs} (i\sigma_x \sigma_y)_{ss'} d_{xz,s'} - p_{z,s} (i\sigma_y \sigma_y)_{ss'} d_{yz,s'} \rangle = g_{2-} \sum_{s,s'} \langle -p_{zs} \sigma_{z,ss'} d_{xz,s'} - ip_{z,s} \sigma_{0,ss'} d_{yz,s'} \rangle, \tag{S5}$$

$$A_{2u} : \Delta_{3+} = g_{3+} \sum_{s,s'} \langle p_{zs} (i\sigma_y \sigma_y)_{ss'} d_{xz,s'} - p_{z,s} (i\sigma_x \sigma_y)_{ss'} d_{yz,s'} \rangle = g_{3+} \sum_{s,s'} \langle ip_{zs} \sigma_{0,ss'} d_{xz,s'} + p_{z,s} \sigma_{z,ss'} d_{yz,s'} \rangle, \tag{S6}$$

$$B_{2u} : \Delta_{3-} = g_{3-} \sum_{s,s'} \langle p_{zs} (i\sigma_y \sigma_y)_{ss'} d_{xz,s'} + p_{z,s} (i\sigma_x \sigma_y)_{ss'} d_{yz,s'} \rangle = g_{3-} \sum_{s,s'} \langle ip_{zs} \sigma_{0,ss'} d_{xz,s'} - p_{z,s} \sigma_{z,ss'} d_{yz,s'} \rangle, \tag{S7}$$

which shows that all gap functions involve pairs with same spins. Based on this, we split the interacting Hamiltonian in two parts

$$H_{int} = H_{0,int} + H'_{int}, \tag{S8}$$

where only $H_{0,int}$ incorporates same-spin pairing terms

$$\begin{aligned}
H_{0,int} = & (V - J_3) \sum_i \left(d_{xz,i\uparrow}^\dagger d_{xz,i\uparrow} p_{z,i\uparrow}^\dagger p_{z,i\uparrow} + d_{xz,i\downarrow}^\dagger d_{xz,i\downarrow} p_{z,i\downarrow}^\dagger p_{z,i\downarrow} \right) \\
& - (J_1 - J_2) \sum_i \left(d_{xz,i\uparrow}^\dagger d_{xz,i\downarrow} p_{z,i\uparrow}^\dagger p_{z,i\downarrow} + d_{xz,i\downarrow}^\dagger d_{xz,i\uparrow} p_{z,i\downarrow}^\dagger p_{z,i\uparrow} \right) \\
& + (V - J_3) \sum_i \left(d_{yz,i\uparrow}^\dagger d_{yz,i\uparrow} p_{z,i\uparrow}^\dagger p_{z,i\uparrow} + d_{yz,i\downarrow}^\dagger d_{yz,i\downarrow} p_{z,i\downarrow}^\dagger p_{z,i\downarrow} \right) \\
& + (J_1 - J_2) \sum_i \left(d_{yz,i\uparrow}^\dagger d_{yz,i\downarrow} p_{z,i\uparrow}^\dagger p_{z,i\downarrow} + d_{yz,i\downarrow}^\dagger d_{yz,i\uparrow} p_{z,i\downarrow}^\dagger p_{z,i\uparrow} \right), \quad (\text{S9})
\end{aligned}$$

In contrast, H'_{int} contains only opposite-spin pairing terms, and is thus not relevant for the current treatment. From the interacting Hamiltonian, it is now straightforward to read off the coupling constants for each superconducting channel:

$$g_{2+} + g_{2-} + g_{3+} + g_{3-} = J_3 - V, \quad (\text{S10})$$

$$g_{2+} + g_{2-} - g_{3+} - g_{3-} = J_2 - J_1. \quad (\text{S11})$$

We therefore obtain

$$g_{2+} + g_{2-} = \frac{-V + J_3 - J_1 + J_2}{2}, \quad (\text{S12})$$

$$g_{3+} + g_{3-} = \frac{-V + J_3 + J_1 - J_2}{2}. \quad (\text{S13})$$

Upon requiring the A_{1u} and B_{1u} channels to be attractive ($g_2 > 0$) and the A_{2u} and B_{2u} channels to be repulsive ($g_3 < 0$), we find the following condition

$$J_3 + J_1 - J_2 < V < J_3 + J_2 - J_1, \quad (\text{S14})$$

which can be satisfied if $J_1 < J_2$ (assuming, as usual, $V > 0$, $J_i > 0$). If we further assume that J_1 , J_2 and J_3 are of the same order $\approx J$, we see that, for this condition to hold, V should generally be of the same order as J . This situation resembles the condition $J > V$ obtained in Ref. [4] to observe s -wave spin-triplet pairing. In this regard, it should be noted that V and J here are not the ‘‘atomic’’ values, but the effective, low-energy values renormalized by high-energy degrees of freedom.

We note that, in order to distinguish between g_{2+} and g_{2-} , additional subleading terms would need to be included in the interacting Hamiltonian. These terms are enabled by the spin-orbit coupling, and thus correspond to terms of the form $\mathbf{L}_i \cdot \mathbf{S}_i$, where $\mathbf{L}_i = \sum_{\alpha\beta ss'} d_{i,\alpha,s}^\dagger \tau_{y,\alpha\beta} \sigma_{ss'} d_{i,\beta,s'}$ and τ acts on the (d_{xz}, d_{yz}) basis. Since these terms are supposed to be subleading due to the moderate value of spin-orbit interaction in the system, we disregard them in our analysis.

-
- [1] Junjiro Kanamori, ‘‘Electron Correlation and Ferromagnetism of Transition Metals,’’ *Progress of Theoretical Physics* **30**, 275–289 (1963), <https://academic.oup.com/ptp/article-pdf/30/3/275/5278869/30-3-275.pdf>.
- [2] Antoine Georges, Luca de’ Medici, and Jernej Mravlje, ‘‘Strong correlations from Hund’s coupling,’’ *Annual Review of Condensed Matter Physics* **4**, 137–178 (2013).
- [3] Siegfried Graser, TA Maier, PJ Hirschfeld, and DJ Scalapino, ‘‘Near-degeneracy of several pairing channels in multiorbital models for the Fe pnictides,’’ *New J. Phys.* **11**, 025016 (2009).
- [4] Oskar Vafek and Andrey V Chubukov, ‘‘Hund interaction, spin-orbit coupling, and the mechanism of superconductivity in strongly hole-doped iron pnictides,’’ *Phys. Rev. Lett.* **118**, 087003 (2017).